

## EFFECT OF NI DOPING ON SOME PROPERTIES OF ELECTRODEPOSITED ZINC ALLOY COATINGS

Malika Diafi <sup>1)\*</sup>, Nadjette Belhamra <sup>1)</sup>, Hachemi Ben Temam <sup>1)</sup>, Brahim Gasmî <sup>1)</sup>, Said Benramache <sup>1)</sup>

<sup>1)</sup> *Physic Laboratory of Thin Films and Applications (LPCMA), University of Biskra, 07000, Algeria*

Received: 23.02.2015

Accepted: 25.08.2015

\*Corresponding author: *e-mail: diafimalika@gmail.com, Tel.: +213557286468, Physic Laboratory of Thin Films and Applications (LPCMA), University of Biskra, 07000, Algeria*

### Abstract

In this work an experimental study Zinc- nickel composite coatings was conducted. For this, the influence of the concentration of Ni is the principal object in order to improve the corrosion resistance of the deposit, which has been made by electroplating on steel substrates previously treated, have been studied by several characterization methods, as the X-ray diffraction, measurement of micro hardness and scanning electron microscopy (SEM), protection against corrosion properties studied in a solution of 3 % NaCl in the potentiodynamic polarization measurements (Tafel), electrochemical impedance spectroscopy (EIS) to the potential of corrosion free. The parameters that characterize the corrosion behavior can be determined from the plots and Nyquist plots. Trends of increasing the charge transfer resistance and the decrease of capacitance values. XRD and SEM results and identify any coatings Zn-Ni alloy composition have similar phase (simple cubic  $\gamma$ -phase structure) and the addition of Ni in the zinc matrix increases the micro-hardness, and we note the maximum hardness is obtained for 0.2M Ni.

**Keywords:** Alloy, Nickel, Zinc, EIS, XRD, SEM.

### 1 Introduction

Electrodeposited zinc (Zn) has been widely used in a variety of applications, including coatings for automotive and electronic parts [1]. Electrodeposited Zn alloys with Fe group metals significantly extend the steel corrosion protection period with respect to conventional Zn coatings [2–5]. Several researchers have attempted to increase the nickel content by either introducing additives in the bath or by developing a ternary alloy [6].

The highest corrosion resistance is achieved when Co or Fe in the alloy is less than 1 wt% and the amount of Ni is within 9–15 wt. % [7]. Electrodeposited Zn–Ni alloys exist in the form of three dominant phases:  $\alpha$ ,  $\gamma$  and  $\eta$ . The  $\alpha$ -phase is a solid solution of Zn in Ni with an equilibrium solubility of about 30 % Zn. The  $\eta$ -phase is a solid solution of Ni in Zn, with a Ni solubility of less than 1 %. The composition range of the pure  $\gamma$ -single phase was determined to be between 10 and 30 % Ni. The amount of Ni in the alloy, which finds industrial application in the corrosion protection field, is around 15% and its dominant structure is the  $\gamma$ -phase  $Zn_{21}Ni_5$  [8]. The purpose of our work is the characterization of composites Zinc-Ni deposits on a mild steel substrate. These deposits are obtained using an acidic sulphate bath, which were introduced

from the suspension ( $\text{NiSO}_4 \cdot 6\text{H}_2\text{O}$ ) with different concentrations. Technical XRD was used for the structure analysis, SEM was used for morphological analysis. Studies potentiodynamic polarization and electrochemical impedance in a solution of 3 % NaCl.

## 2 Experimental

### 2.1 Coating processes

The deposition of Zn–Ni coatings was carried out onto steel substrates under galvanostatic conditions at operating current density of  $10 \text{ A dm}^{-2}$  and a temperature of  $30 \text{ }^\circ\text{C}$ . The chemical composition of the basic electrolyte of pure Zn coating the plating bath alloys deposition was given in **Table 1** [3,6,9,]. Electrodeposits Zn were obtained by varying the concentration of Ni in the bath (0.05, 0.1, 0.15 0,2 M).

### 2.2 Coating characterization

XRD characterization of samples was carried out with a D8 Advance–Bruker using a Cu  $K\alpha$  line at  $\lambda = 0.1540 \text{ nm}$  in the  $2\theta$  ranged of  $10\text{--}95^\circ$  in steps of  $0.02^\circ$  at a scan speed  $2^\circ/\text{min}$ . Bruker GAADS soft-ware was utilized to calculate.

**Table 1** Electrolyte I composition and conditions for alloy plating.

Electrolyte I Ingredients	Concentration ( $\text{g}\cdot\text{l}^{-1}$ )	Plating parameters
$\text{ZnSO}_4 \cdot 7\text{H}_2\text{O}$	57.5	30 °C and pH=3-4,5 constant current densities at 10 mA $\text{cm}^{-2}$ for 60 s
$\text{H}_3\text{BO}_3$	9.3	
$\text{Na}_2\text{SO}_4$	56.8	
$\text{Na}_3\text{C}_6\text{H}_5\text{O}_7$	56.8	

the biaxial stress along the lateral and longitudinal directions with 2D area detector using a standard  $2\theta \sin 2\psi$  method [10]. The average grain size of the coatings was determined from X-ray peak broadening by applying the Scherrer formula [11,12]:

$$D = \frac{0.9\lambda}{\beta \cos \theta} \quad (1.)$$

where  $D$  is the grain size,  $\lambda$  is the X-ray wavelength ( $\lambda = 1.5406 \text{ \AA}$ ),  $\beta$  is the full width at half-maximum (FWHM), and  $\theta$  is Bragg angle position of peak. For (330) reflections and peak broadening was measured by the integral width method [13]; Surface morphology of the deposits was followed with A JEOL (model JSM6390LV),

Microhardness of coatings was measured using a load of 100 g with a holding time of 15 s by using a Vickers hardness tester(HV) of deposits were performed in the surface by using a Wolpert Wilson Instruments (model 402UD) [14].

### 2.3 Corrosion testing

Corrosion behavior and protection performance of Zn–Ni alloy coatings was studied by using electrochemical impedance spectroscopy (EIS) and electrochemical Tafel extrapolation in 3 wt. % NaCl solution. The tests were performed using a potentiostat /ga- Ivanostat (using a Volta Lab

40), The working electrode was a coated sample, the counter electrode was platinum with an area of  $1 \text{ cm}^2$  and the reference electrode was Hg/HgO/ 1 M KOH. All potentials in the text have been referred to this reference electrode. Electrochemical impedance spectroscopy (EIS) measurements were obtained at the open circuit potential (OCP) in a frequency range of 10 kHz–0.001 Hz, with an applied AC signal amplitude perturbation of 10 mV. During the measuring process of Tafel polarizing curves, the polarization curve scanning rate was 5 mV/s, with a scanning range from  $-0.25 \text{ V}$  of open circuit potential to  $+0.25 \text{ V}$  of open circuit potential. The  $E_{\text{Corr}}$  and  $I_{\text{Corr}}$  were determined from the intercepts by Tafel extrapolation method.

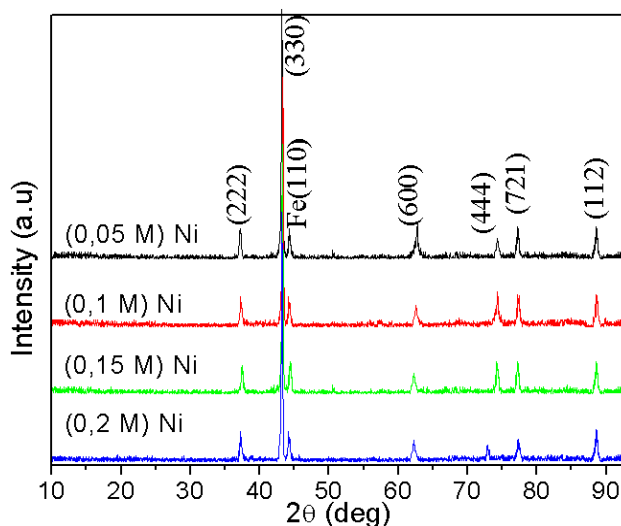


**Fig. 1** XRD patterns of Zn–Ni alloy coatings electrodeposited at different concentrations of Ni

### 3 Results and discussions

#### 3.1 X-ray diffraction

x-ray diffraction patterns of the coatings obtained at different current densities are shown in **Fig. 1**. According to Zn–Ni phase diagram and past researches [13,15–18], electrodeposited Zn–Ni alloys have four main phases:  $\alpha$ -phase, a solid solution of zinc in nickel with an equilibrium solubility of about 30% Zn;  $\gamma$ -phase, an inter-mediate phase with a composition  $\text{Ni}_5\text{Zn}_{21}$ ;  $\delta$ -phase, an intermediate phase with a composition  $\text{Ni}_3\text{Zn}_{22}$ ; and  $\eta$ -phase, a solid solution of nickel in zinc with less than 1% nickel. X-ray analysis was done for all deposits and the results show that all coatings have only a single cubic  $\gamma$ -phase structure ( $\text{Ni}_5\text{Zn}_{21}$ ), from  $\gamma$ - ( $\text{Ni}_5\text{Zn}_{21}$ ) phase increases with increasing Ni concentration [19–21].

#### 3.2 Morphologies registered electro layers

The morphology of these coatings plated in different compositions is presented in **Fig. 2**. The deposit is rough, contains some pores, with less-uniform surface and the grain size is about 45.3 nm at 0.05 M  $\text{Ni}^{2+}$  and 42.3 nm at 0.1M  $\text{Ni}^{2+}$  concentrations in the bath (Fig. 2a) and (Fig. 2b). This is probably due to the higher Zn content in the deposited film with respect to nickel. Increasing  $\text{Ni}^{2+}$  concentration in the bath to 0.15M and 0.2 M gives a uniform (homogeneous),

small grain size (about 33.6 nm and 29.2 nm respectively) and compact deposit (Fig. 2c) and (Fig. 2d). This is not only due to the increase of Ni content in the deposit but also due to the slight increase in cobalt content. Also, it was stated that the decrease in grain size result in an improvement of passive film's protective performance and thus, increasing the corrosion resistance [19, 22].

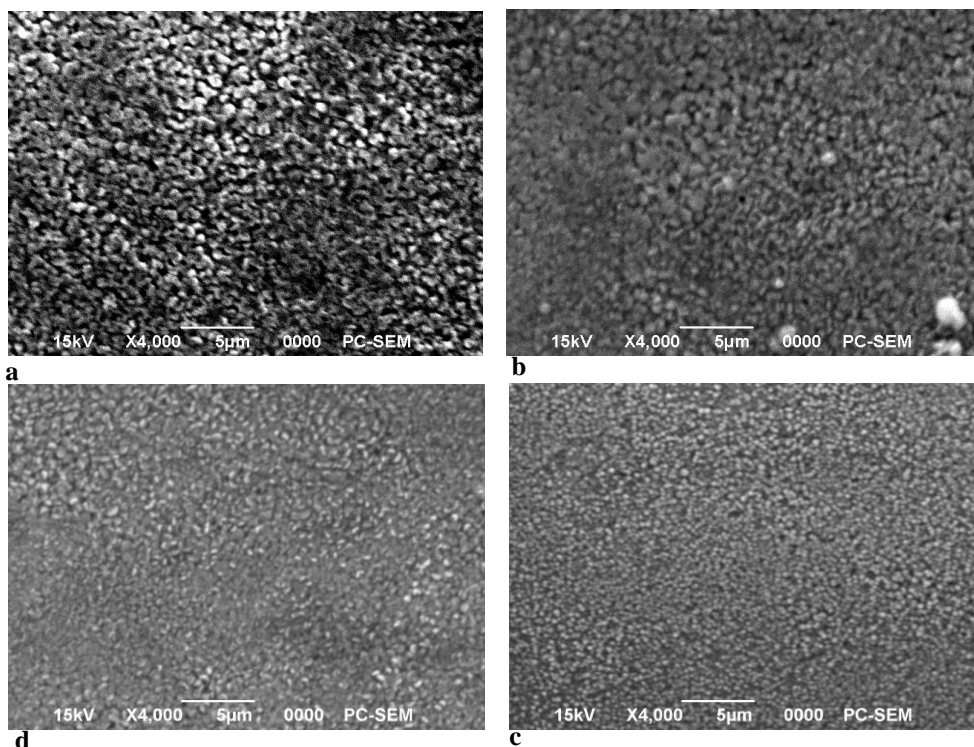


**Fig. 2** Surface morphology of Zn–Ni alloy coatings electrodeposited with different concentrations of Ni: (a): 0.05 M, (b): 0.1 M, (c): 0.15 M and (d): 0.2 M

**Table 2** Values of micro-hardness Vickers hardness (HV) registered different electro deposition

Coating	Dureté (HV)
Steel	167.7
Zn (0,2M) + (0,05M) Ni	175
Zn (0,2M) + (0,1M) Ni	200
Zn (0,2M) + (0,15M) Ni	217.7
Zn (0,2M) + (0,2M) Ni	246

### 3.3 The method of micro-hardness

Control measures the mechanical properties of Zn electro layers deposited in the presence of Ni, which were summarized in **Table 2** and **Fig. 3**.

These results show that the coatings prepared from the bath have chosen good hardness, and the addition of Ni in the zinc matrix increases micro-hardness, This is because that the hardness of

Ni is greater than Zn, higher Ni content in the coating provided higher hardness, and we note the maximum hardness is obtained for 0,2M Ni. The presence of smaller grains impedes dislocation motion and results in an increase in microhardness [14,23].

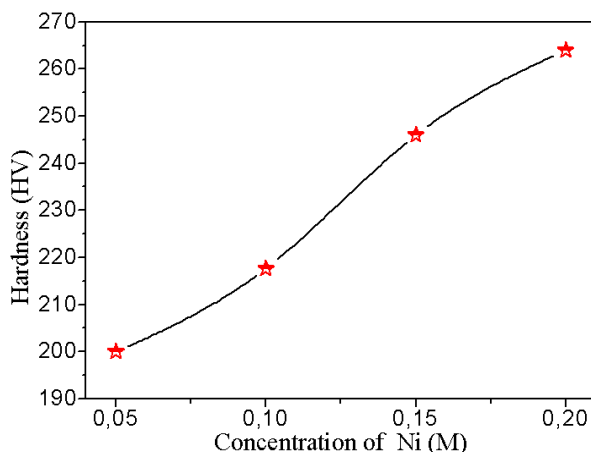
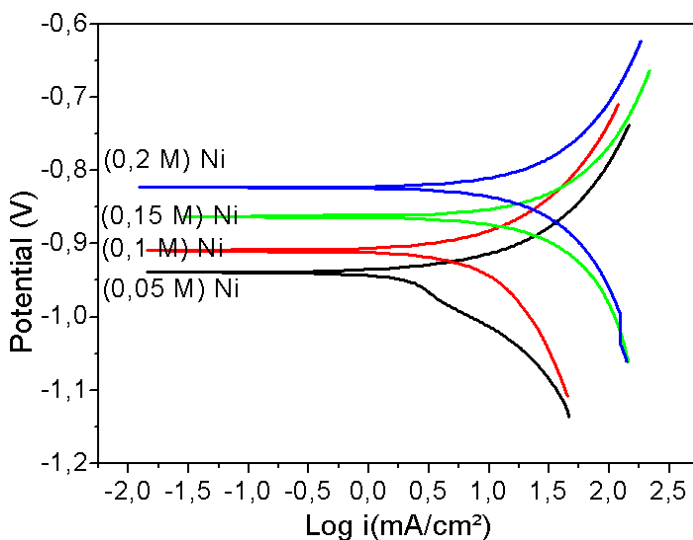


**Fig. 3** Change in hardness micro electro composite coatings deposited depending on the concentration of Ni

### 3.4 Corrosion studies

#### 3.4.1. Potentiodynamic polarization studies

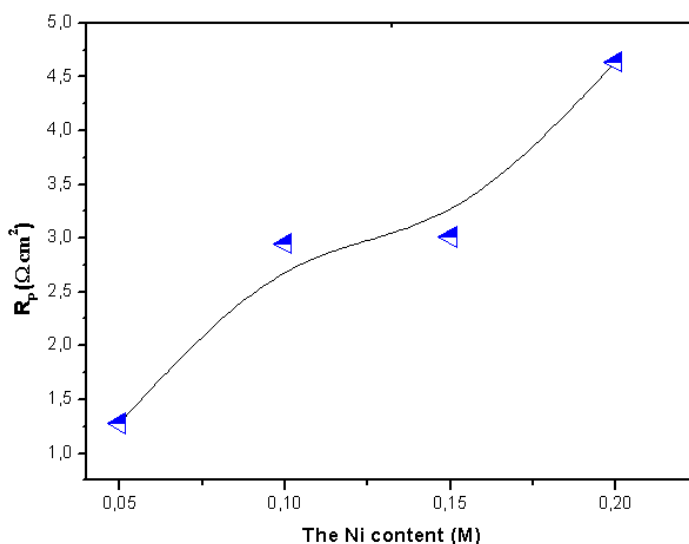
The corrosion resistance of the deposits was determined by measuring the potentiodynamic polarization curves (**Fig. 4**). These curves were obtained for Zn–Ni–Co alloys that deposited on steel rod from sulphate bath at different Ni<sup>2+</sup> concentrations, in aerated 3 wt. % NaCl solution. The corrosion potential  $E_{corr}$ , the polarization resistance  $R_p$  and corrosion current ( $i_{corr}$ ). Values were determined from this figure and cited in **Table 3**.



**Fig. 4** Polarizing curves obtained for the alloy coatings in a 3 % NaCl solution at different concentrations of Ni

**Table 3** The electrochemical parameters ( $E_{corr}$ ,  $I_{Corr}$ ,  $\beta_a$ ,  $\beta_c$ ) of the coatings samples in a 3 % NaCl solution

Coating	$E_{corr}$ (mV)	$I_{Corr}$ (mA/cm <sup>2</sup> )	$\beta_a$ (mV/dec)	$\beta_c$ (mV/dec)
Zn (0,2M) + (0,05M) Ni	-939	42,24	282	-108,04
Zn (0,2M) + (0,1M) Ni	-909	39,15	252,2	-318,9
Zn (0,2M) + (0,15M) Ni	-823	13 ,57	181, 3	-373,8
Zn (0,2M) + (0,2M) Ni	-863	32 ,20	116 ,7	-338,8

**Fig. 5** The variation of polarization resistance ( $R_p$ ) of concentration Ni.

Variation of polarization resistance ( $R_p$ ) of Zn–Ni alloy coatings versus the concentration of Ni presented in Fig.5. The addition of Ni in Zn–Ni alloys increases the deposit's corrosion resistance [24,25]. Increasing the  $\text{Ni}^{2+}$  concentration in the plating bath increases the corrosion resistance of the deposit. This may be due to the increase in the  $\gamma$ -phase and decrease in the pure Zn phase of the alloy. Also the surface morphology of the deposits was improved with increasing  $\text{Ni}^{2+}$  concentration [19].

### 3.4.2. Electrochemical impedance spectroscopy (EIS) studies

Electrochemical impedance spectroscopy (EIS) is well-established and powerful technique in the study of corrosion. Surface properties, electrode kinetics and mechanistic information can be obtained from impedance diagrams. We can studied an equivalent circuit by deriving its impedance equation. However, it's simpler to perform a measurement on the circuit and analyze the resulting plot. We'll get a good picture of the real and imaginary impedance components and of the phase shift characteristics as a function of frequency. The Randles cell (see **Fig. 6**) models the electrochemical impedance of an interface and fits many chemical systems. We can easily equate the circuit components in the Randles cell with familiar physical phenomena, such as adsorption or film formation  $R_s$  is the ohmic or uncompensated resistance of the solution between the working and reference electrodes.  $R_p$  is the polarization resistance or charge transfer

resistance at the electrode/solution interface. ( $C_{dl}$  or  $Q_{dl}$ ) is the double layer capacitance at this interface. The double layer capacitance is replaced by the term  $Q$  which is called the constant phase element [17]. The impedance is then given by the Eq. (2) [16].

$$Z_Q = [Y_0 J \omega^{-n}]^{-1} \quad (2.)$$

where  $Z$  is the impedance ( $\Omega$ ),  $Y_0$  is the capacitance factor ( $\Omega^{-1} \text{sn}$ ),  $\omega$  is the angular frequency ( $\text{rad S}^{-1}$ ), and  $n$  is the empirical exponent of  $Q$ . When  $Q$  is close to 1 the behavior can be equalized to a double layer capacitance. In a Nyquist plot the polarization resistance approximately corresponds to the size of the semicircle [10].

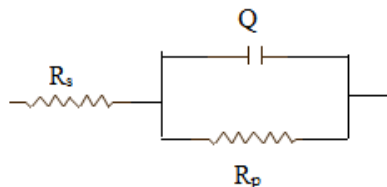


**Fig. 6** Equivalent Circuit for a Single Electrochemical Cell.

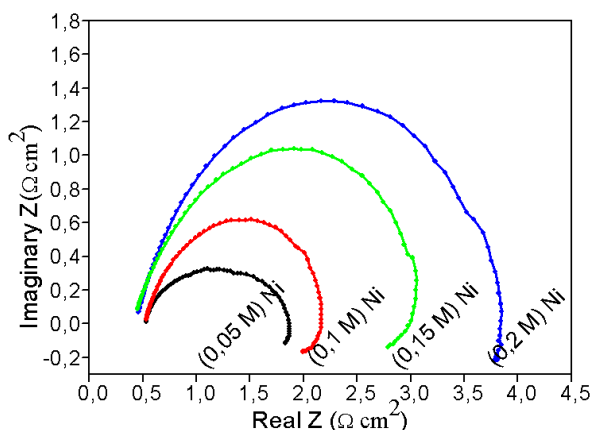


**Fig. 7** The Nyquist plots obtained for Zn-Ni alloy coatings electrodeposited at different concentrations of Ni.

EIS studies have been performed in 3 wt. % NaCl solution to evaluate corrosion resistance behavior of the samples. As seen in **Fig. 7**, Nyquist responses of all samples are in depressed semicircle (unfinished) shape. The diameter of this semicircle reflects the corrosion resistance of the related sample. As can be seen, the semicircle diameter of the sample obtained at 0,2 M Ni is the biggest and the semicircle diameter of sample obtained at 0,05 M Ni is the lowest one (The increase in the size of the capacitive loop with the addition of Ni). So the highest corrosion resistance was obtained in the sample of 0,2 M Ni and the lowest one was also obtained for 0,05 M, these results are consistent with the polarization studies. The real parts of the impedance of the samples are significantly bigger than the imaginer part. This can be attributed to the charge transfer resistance control of the corrosion reactions of the samples because of the domination of Zn-rich phases in the coatings. Extracted fitted data from the equivalent circuit is shown in **Table 4**.

results shown in the **Table 4**, the value of  $R_t$  increase with increase in the concentration of Ni and decrease in  $C_{dl}$ . As seen in Bode curves **Fig. 8**, the maximum phase angle can be seen in the sample obtained at 0,2 M Ni and has a larger maximum phase angle margin compared to the others samples. This fact shows that this sample has the highest barrier property. This can be attributed to the higher Ni amount, grain uniformity and surface coverage of this deposit. The negative phase angle seen in high frequency region can be attributed to dehydration reaction on the surface. The EIS data reveal that the sample obtained at 0,2 M Ni has the best corrosion protection performance. This result is consistent with the potentiodynamic polarization studies (see **Fig. 4**).

**Table 4** Extracted fitted data from the equivalent circuit of Zn–Ni alloy coatings in a 3 % NaCl solution

Coating	$R_p$ ( $\Omega \cdot \text{cm}^2$ )	$R_s$ ( $\Omega \cdot \text{cm}^2$ )	$C_{dl}$ ( $\mu\text{F}/\text{cm}^2$ )
Zn (0,2M) + (0,05M) Ni	1,28	0,46013	0,232
Zn (0,2M) + (0,1M) Ni	2,95	0,46845	0,2281
Zn (0,2M) + (0,15M) Ni	3,01	0,5293	0,2019
Zn (0,2M) + (0,2M) Ni	4,64	0,53417	0,200

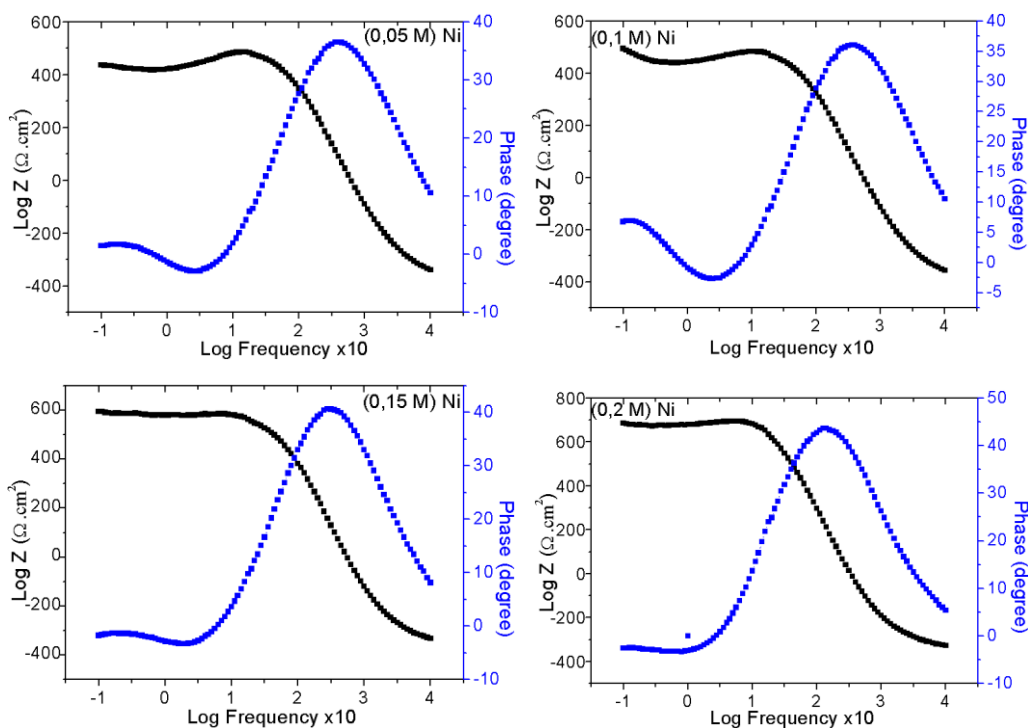


**Fig. 8** The Bode plots obtained for NC Zn–Ni alloy coatings electrodeposited at different concentrations of Ni

#### 4 Conclusion

The following conclusions were drawn:

- Adherent alloy coatings light, compact and good were obtained with galvanostatic conditions. XRD and SEM results indicate all the Zn-Ni alloy coatings have similar composition phase (simple cubic  $\gamma$ -phase structure), Increasing the  $\text{Ni}^{2+}$  concentration in the plating bath increases the  $\gamma$ -phase and decrease in the pure Zn phase of the alloy. [21]
- The test of the micro-hardness on the various electro deposited coatings has a maximum value (0.2 M) Ni, because the increase of the  $\text{Ni}^{2+}$  concentration in the plating bath increases of micro-hardness.
- Also the surface morphology of the deposits was improved with increasing  $\text{Ni}^{2+}$  concentration, gives a more uniform surface morphology and more compact deposits.
- The study by the method from potentiodynamic polarization curves showed that the values of the corrosion current density ( $I_{corr}$ ) decreases, the corrosion potential ( $E_{corr}$ ) and the polarization resistance ( $R_p$ ) increases with increasing the concentration of Nickel in the electrolyte bath.
- EIS analysis performed on the developed coatings that have increased resistors  $R_s$ . The Increase in the size of the capacitive loop with the addition of Ni.

## References

- [1] Y. Boonyongmaneerat, S. Saenapitak, K. Saengkiettiyut: Journal of Alloys and Compounds, Vol. 487, 2009, No. 1-2, p. 479–482, DOI:10.1016/j.jallcom.2009.07.163
- [2] L.S. Tsybul'skaya, T.V. Gaev'skaya, O.G. Purov'skaya, T.V. Byk: Surface and Coatings Technology, Vol. 203, 2008, No. 1, p.234–239, DOI:10.1016/S0257-8972(00)00934-8
- [3] A. Tozar, I.H. Karahan: Applied Surface Science, Vol. 318, 2013, p. 15–23, DOI:10.1016/j.apsusc.2013.12.020
- [4] R. Fratesi, G. Roventi, G. Giuliani, C.R. Tomachuk: Journal of Applied Electrochemistry, Vol. 27, 1997, No. 9, p. 1088–1094, DOI:10.1023/A:1018494828198
- [5] I.H. Karahan, H.S. Guder: Transactions of the Institute of Materials Finishing, Vol. 87, 2009, No. 3, p. 155–158, DOI:10.1179/174591909X438875
- [6] O. Hammami, L. Dhouibi, P. Berçot, E. Rezzazi: Surface & Coatings Technology, Vol. 219, 2013, p. 119–125, DOI:10.1016/j.surfcoat.2013.01.014
- [7] R. Ramanauskas, R. Juskenas, A. Kalinichenko, L. F. G. Mesias: Journal of Solid State Electrochemistry, Vol.8, 2004, No. 6, p 416–421, DOI:10.1007/s10008-003-0444-2.
- [8] R. Ramanauskas, L. Gudaviciut, A. Kalinichenko, R. Juskenas: Journal of Solid State Electrochemistry, Vol. 9, 2005, No. 12, p. 900–908, DOI:10.1007/s10008-005-0049-z
- [9] O. Hammami, L. Dhouibi, P. Berçot, M. Rezzazi, E. Triki: Surface & Coatings Technology, Vol. 203, 2009, No. 19, p. 2863–2870, DOI:10.1016/j.surfcoat.2009.02.129.
- [10] K.R. Sriraman, S. Brahimi, J.A. Szpunar, J.H. Osborned, S. Yue: Electrochimica Acta, Vol. 105, 2013, p. 314– 323, DOI:10.1016/j.electacta.2013.05.010
- [11] F.Z. Lemmadi, A. Chala, O. Belahssen, S. Benramache: Acta Metallurgica Slovaca, Vol. 20, 2014, No. 4, p. 375-380, DOI:10.12776/ams.v20i4.354
- [12] S. Benramache, B. Benhaoua, O. Belahssen: Optik, Vol. 125, 2014, No. 19, p. 5864-5868, DOI:10.1016/j.ijleo.2014.07.055
- [13] S.H. Mosavat, M.H. Shariat, M.E. Bahrololoom: Corrosion Science, Vol. 59, 2012, p. 81–87, DOI:10.1016/j.corsci.2012.02.012
- [14] S. Ghaziof, W. Gao: Journal of Alloys and Compounds, Vol. 622, 2015, p. 918–924, DOI:10.1016/j.jallcom.2014.11.025

- [15] D.E. Hall: plating and surface finishing, Vol. 70, 1983, p. 59–65
- [16] L.S. Tsybul'skaya, T.V. Gaev'skaya, O.G. Purov'skaya, T.V. Byk: Surface & Coatings Technology, Vol. 203, 2008, No. 3-4, p. 234–239, DOI:10.1016/j.surfcoat.2008.08.067
- [17] F. Mansfeld: Corrosion, Vol. 37, 1981, No. 5, p. 301–307, DOI:10.5006/1.3621688
- [18] L.M. Chang, D. Chen, J.H. Liu, R.J. Zhang: Journal of Alloys and Compounds, Vol. 479, 2009, No. 1-2, p. 489–493, DOI:10.1016/j.jallcom.2008.12.108
- [19] M.M. Abou-Krishna: Materials Chemistry and Physics Vol. 125, 2011, No. 3, p. 621–627, DOI:10.1016/j.matchemphys.2010.10.007
- [20] Z. Wu, L. Fedrizzi, P.L. Bonora: Surface & Coatings Technology, Vol. 85, 1996, No. 3, p. 170–174, DOI:10.1016/0257-8972(96)02857-5
- [21] T.L. Ramachar, S.K. Panikkar: Electroplating Metal Finishing, Vol. 13, 1960, p. 405–412
- [22] Kh.M.S. Youssef, C.C. Koch, P.S. Fedkiw: Corrosion Science, Vol. 46, 2004, No. 1, p. 51–64, DOI:10.1016/S0010-938X(03)00142-2
- [23] A.M. Alfantazi, U. Erb: Materials Science and Engineering A, Vol. 212, 1996, No. 1, p. 123–129, DOI:10.1016/0921-5093(96)10187-8
- [24] M.E. Soares, C.A.C. Souza, S.E. Kuri: Surface & Coatings Technology, Vol. 201, 2006, No. 6, p. 2953–2959, DOI:10.1016/j.surfcoat.2006.06.006
- [25] J.R. Vilche et al.: Journal of The Electrochemical Society, Vol. 136, 1989, No. 12, p. 3773–3779, DOI: 10.1149/1.2096546

### **Acknowledgments**

*I would like to thank "Responsible of Physics Laboratory of Thin Films and Applications (LPCMA)" for their assistance in the preparation of this work.*